Electronic Supplementary Material (ESI) for Environmental Science: Nano.
This journal is © The Royal Society of Chemistry 2019

Supplementary Information

Roles of extracellular polymeric substances in bactericidal effect of nanoscale zero-valent iron: Trade-offs between physical disruption and oxidative damage

Ying Hu [a, b, #], Jian Wang [c, #], Hongwei Sun [a, d, *], Shaohui Wang [c], Xiaomei Liao [c], Jun Wang [b, e, *], Taicheng An [f]

[a] Key Laboratory of Pesticide & Chemical Biology of Ministry of Education, Institute of Environmental Chemistry, College of Chemistry, Central China Normal University, Wuhan 430079, P. R. China

[b] Key Laboratory of Aquatic Botany and Watershed Ecology, Wuhan Botanical Garden, Chinese Academy of Sciences, Wuhan 430074, China

[c] Hubei Key Lab of Genetic Regulation and Integrative Biology, School of Life Sciences, Central China Normal University, Wuhan 430079, P. R. China

[d] Division of Environmental Science and Engineering, Pohang University of Science and Technology (POSTECH), Pohang 37673, Korea

[e] Sino-Africa Joint Research Center, Chinese Academy of Sciences, Wuhan, 430074, China

[f] Guangzhou Key Laboratory Environmental Catalysis and Pollution Control, Guangdong Key Laboratory of Environmental Catalysis and Health Risk Control, School of Environmental Science and Engineering, Institute of Environmental Health and Pollution Control, Guangdong University of Technology, Guangzhou 510006, China

[#] Y. H. and J. W. contribute equally to this work.

* To whom correspondence should be addressed.

E-mail: sunhw@mail.ccnu.edu.cn (H. S.); wangjun@wbgcas.cn (J. W.)

24 pages, 8 text, 15 figures, 2 tables

CONTENTS

Text S1. Synthesis and characterization of nanoscale zero-valent iron (nZVI)

Nanoscale zero-valent iron was prepared by reducing the ferrous ion with borohydride. First, $FeSO_4 \cdot 7H_2O$ (9.73 g) was dissolved in 200 mL of 20% ethanol water solution (1:4, v/v). Then, a freshly prepared $NaBH_4$ solution (1.8 g of $NaBH_4$ in 200 ml of N_2 saturated distilled water) was added into the above ferrous solution at the rate of 1-2 drops per second with constant stirring at room temperature under protection of N_2. Once all the $NaBH_4$ solution was added, the mixture was continuously stirred for another 30 min. The nZVI was harvested by centrifugation at 4000 rpm for 4 min and washed 3 times with deoxygenated distilled water and ethanol, and further dried in nitrogen atmosphere.

The morphology and size of the as prepared nZVI were characterized by using transmission electron microscope (TEM, Philips CM12). X-ray powder diffraction (XRD, Bruker AXS D8-FOCUS, Germany) analysis of freshly synthesized nZVI was performed with Cu Kα radiation (λ=1.54184 Å) and graphite monochromator at voltage of 40 kV and current of 40 mA. The scan was in the 2 theta angle (2θ) range of 10°-90° with a step length of 0.02° at 8°/min.

Text S2. Measurement of intracellular reactive oxygen species (ROSs) concentrations

Five milliliter of slurry sample was taken from the nZVI-*E. coli* systems at predetermined time and 5 μL of 25 mM DCFH-DA was added. The thoroughly mixed solution was incubated for 20 min at 37 °C under dark condition. After that, cells were collected by filtration and washed twice with 0.85% NaCl, then the cells were resuspended in 200 μL 0.85% NaCl. The fluorescent was measured using a plate reader (excitation at 488 nm and emission at 525 nm).

Text S3. Membrane potential measurement

Rhodamine 123 (Rh123) was used to measure the membrane potential of *E. coli*. Briefly, five milliliters of bacterial suspension were collected from the nZVI-*E. coli* systems at each sampling point, and 50 μL 1 mg/mL Rh123 solution in DMSO was added quickly. The mixture was incubated for 30 min at 37 ºC in the dark, then the *E. coli* cells were harvested and washed twice with 0.85% NaCl. The resulting samples was resuspended in 200 μL 0.85% NaCl and the fluorescent intensity determined at wavelength of 529 nm with excitation wavelength of 507 nm.

Text S4. Measurement of adenosine triphosphate (ATP) biosynthesis rate

Aliquots of 5 mL samples were collected at 0, 15, 30, 45 and 60 min and mixed with 0.1 mL of fresh LB nutrient broth to incubate at 37 ºC in an orbital shaker. After incubation for 5, 15, 30, 45 and 60 min, the concentrations of ATP were measured with a BacTiter-Glo™ Microbial Cell Viability Assay Kit (G8230, Promega Corporation) following the manufacturer's protocol. Briefly, 0.05 mL *E. coli* culture was mixed with 0.05 mL BacTiter-Glo™ reagent and the luminescence intensity was recorded after 5 min on a plate reader (Varioskan Flash, Thermo Scientific, USA). ATP-2Na·3H_2O standard solution was assayed by identical procedures to construct the calibration curve of ATP concentrations. ATP concentration was plotted against incubation time, and linear fit of the data was made. Slope of the regression line represented the rate of ATP biosynthesis by *E. coli* cells.

Text S5. Bacterial sample preparation protocol for SEM

Cells after nZVI treatment were harvested by centrifugation and fixed with 2.5% glutaraldehyde overnight at ambient temperature. Then the samples were centrifuged at 8000 rpm for 2 min to collect the cells, which were subsequently soaked in 0.1% phosphate-buffered saline (PBS) for 20 min, and centrifuged again. Repeat this procedure 6 times, and the resulting pellet was dehydrated by

soaking the sample sequentially in 30, 50, 70 and 90% ethanol for 15 min, 100% ethanol for 15 min and 3 times, and finally 100% tert-butyl alcohol for 15 min and 3 times. The samples were freeze dried and sputtered with Au for SEM characterization.

Text S6. *E. coli* sample preparation protocol for TEM

A drop of the sample containing *E. coli* cells and nZVI was added onto a glow-discharged Formvar-coated copper grid, and the excess liquid was removed by using filter paper after 2 min. Then the grids were further stained with 1% phosphotungstic acid for another 2 min, and the residual staining solution was drained off. The samples were transferred into TEM chamber instantly, and inspected at accelerating voltage of 200 kV.

Text S7. Characterization of used nZVI samples

The slurry samples composed of *E. coli* and nZVI after different contact duration were collected by vacuum filtration, washed with deionized water to remove residual buffer solution, and freeze-dried. The obtained samples were characterized with a JEOL JSM 7401F high resolution field emission scanning electron microscope (FESEM) at 20.0 kV. XRD (Bruker AXS D8-FOCUS, Germany) analysis of the same samples was performed with Cu Kα radiation (λ=1.54184 Å) in the 2 theta angle (2θ) range of 10°-80°. Fourier-transform infrared spectroscopy (FT-IR, Nicolet iS50) analysis was performed using KBr discs, and the spectrum width was 400-4000 cm^{-1} with a step of 2 cm^{-1}. X-ray photoelectron spectroscopy (XPS, PHI X-tool, DE) data were recorded with the Al Kα line at 15 kV and 51W.

Text S8. Recovery test of membrane integrity after nZVI inactivation

The *E. coli* cells after 30 and 60 min of nZVI (500 mg/L) inactivation were harvested and resuspended in fresh sterilized LB medium, followed by dark incubation in an orbital shaker at 37 ºC and 200 rpm. Samples were withdrawn at regular time intervals (0, 0.5, 1, 1.5 and 2 h) during the incubation, which were stained with LIVE/DEAD™ BacLight™ Bacterial Viability Kit for 15 min in the dark, and then characterized by using the fluorescence microscope.

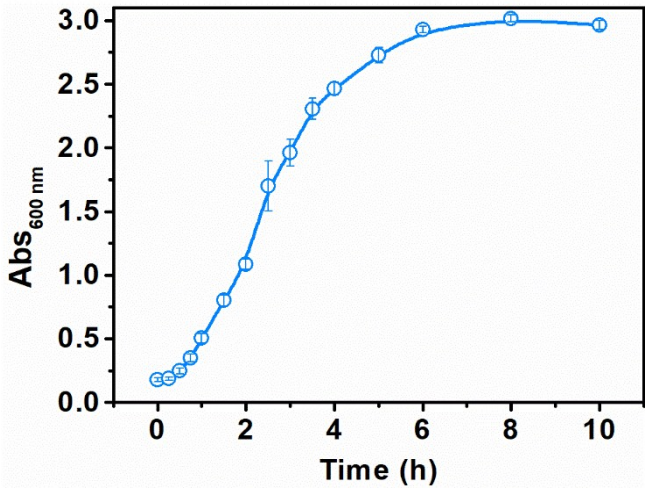

Figure S1. The growth curve of *E. coli* BW25113. Condition: the bacteria cultured overnight in Luria-Bertani (LB) broth medium (10 g/L tryptone, 5 g/L yeast extract and 5 g/L NaCl, pH 7.0) were diluted with 50 mL fresh LB broth, and incubated at 37 °C and 200 rpm.

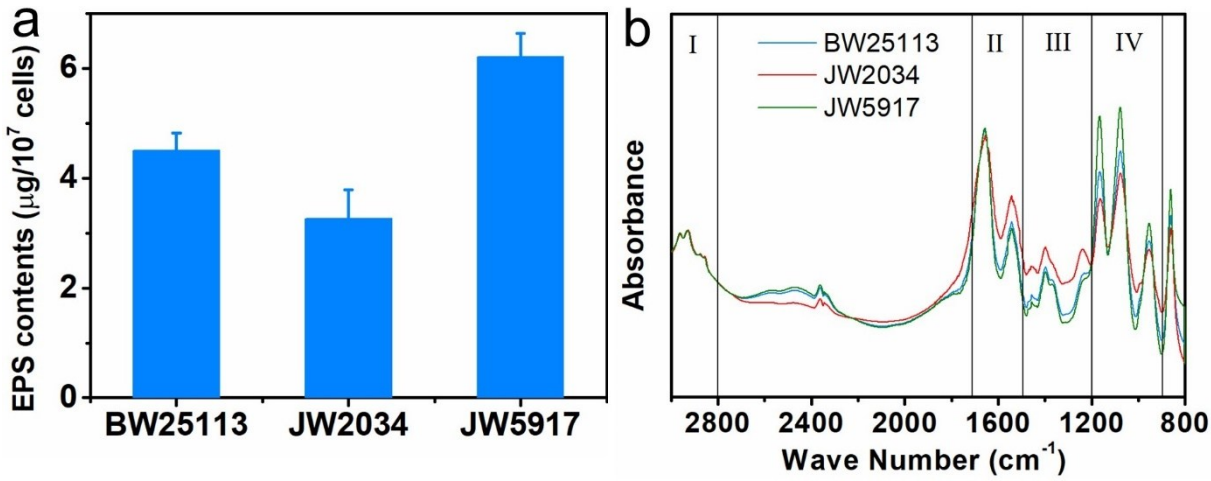

Figure S2. (a) Capsular EPS contents of parental and mutant *E. coli* strains. (b) Normalized FT-IR spectra of the three *E. coli* strains.

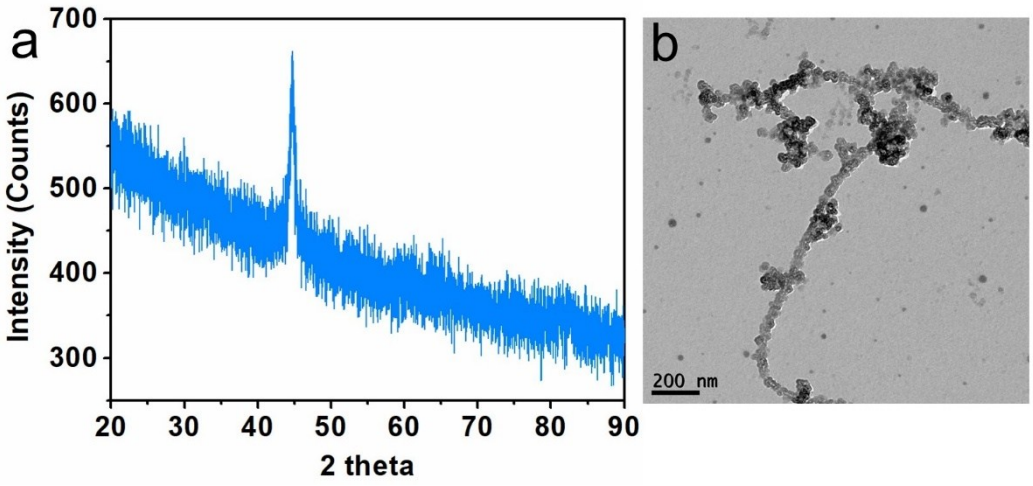

Figure S3. (a) XRD pattern and (b) typical TEM image of the as-prepared nZVI samples.

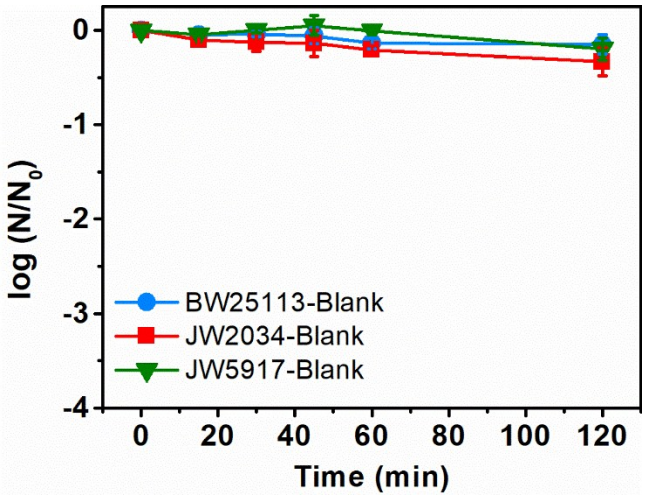

Figure S4. Control experiments of *E. coli* inactivation in the absence of nZVI.

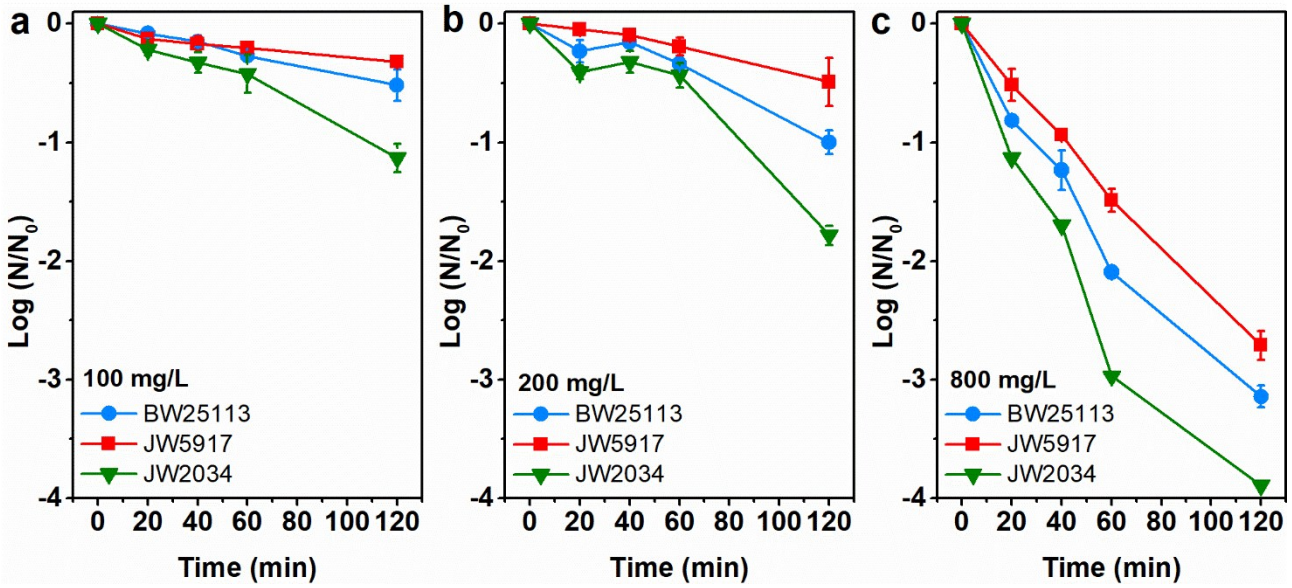

Figure S5. Inactivation of parental *E. coli* BW25113 and mutant strains at different nZVI doses. (a) 100 mg/L, (b) 200 mg/L and (c) 800 mg/L.

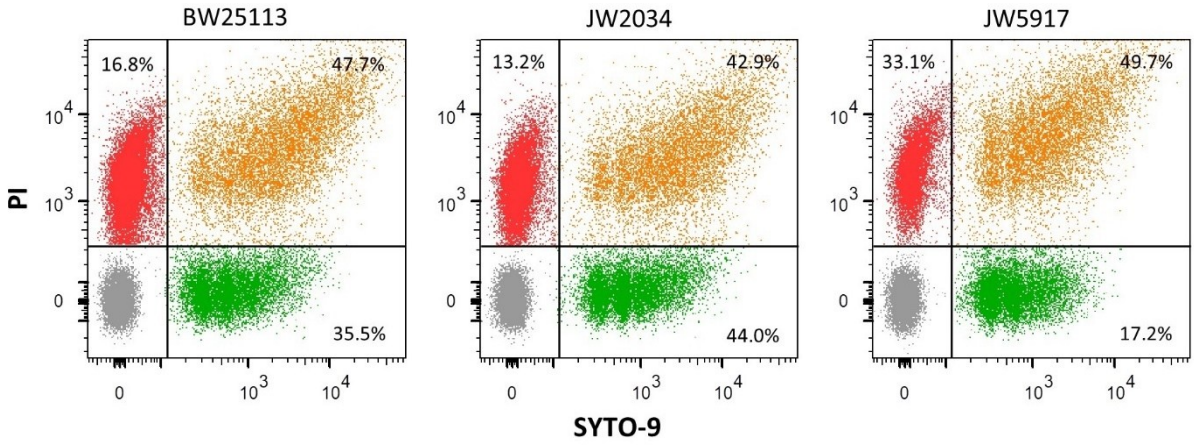

Figure S6. Flow cytometer dot plots (fluorescent intensity of PI vs. SYTO 9) of bacterial samples after 15 min of nZVI inactivation. The plots were classified into 4 clusters, i.e., red (PI+, SYTO 9−) ascribed to cells with permeable membrane, orange (PI+, SYTO 9+) ascribed to cells with partially permeable membrane, green (PI−, SYTO 9+) ascribed to cells with intact membrane and grey (PI−, SYTO 9−) ascribed to background signals. Background signals were not included when calculating the fractions of different clusters. The dose of ZVI was 500 mg/L.

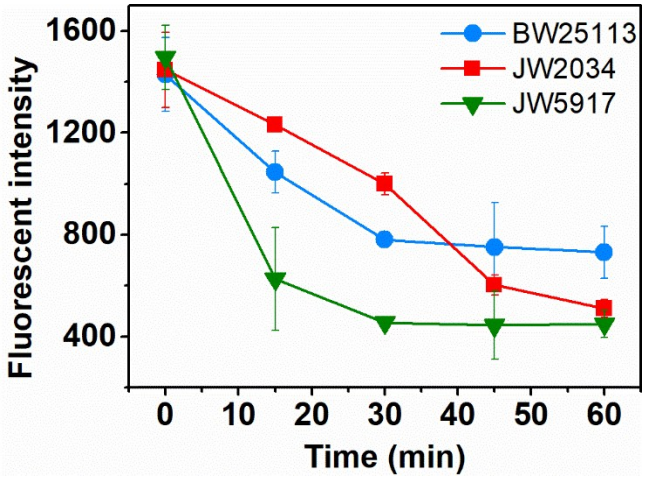

Figure S7. Membrane potential of *E. coli* during nZVI inactivation, determined by using Rh123 as a fluorescence probe.

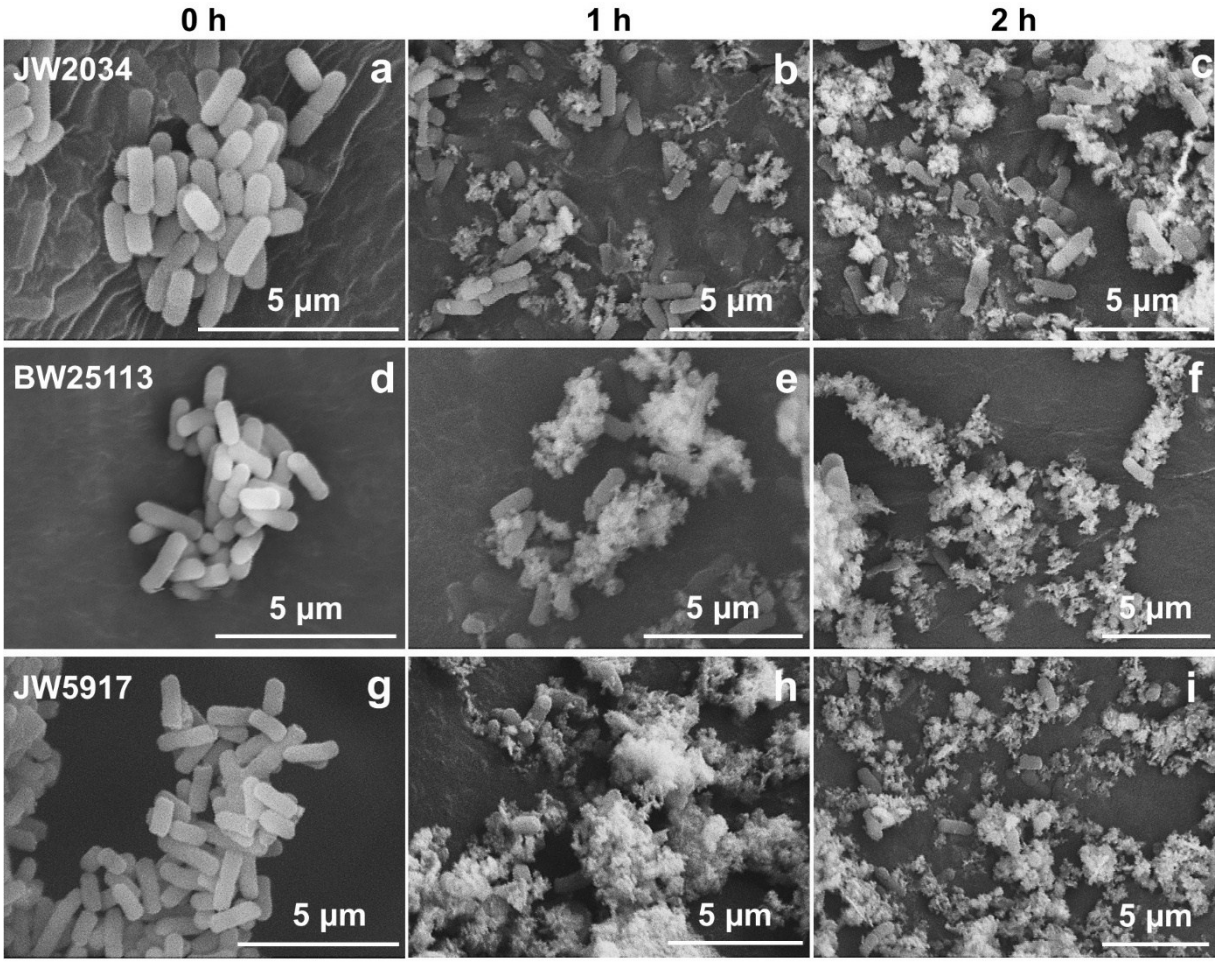

Figure S8. SEM images of *E. coli* cells after different duration of nZVI inactivation.

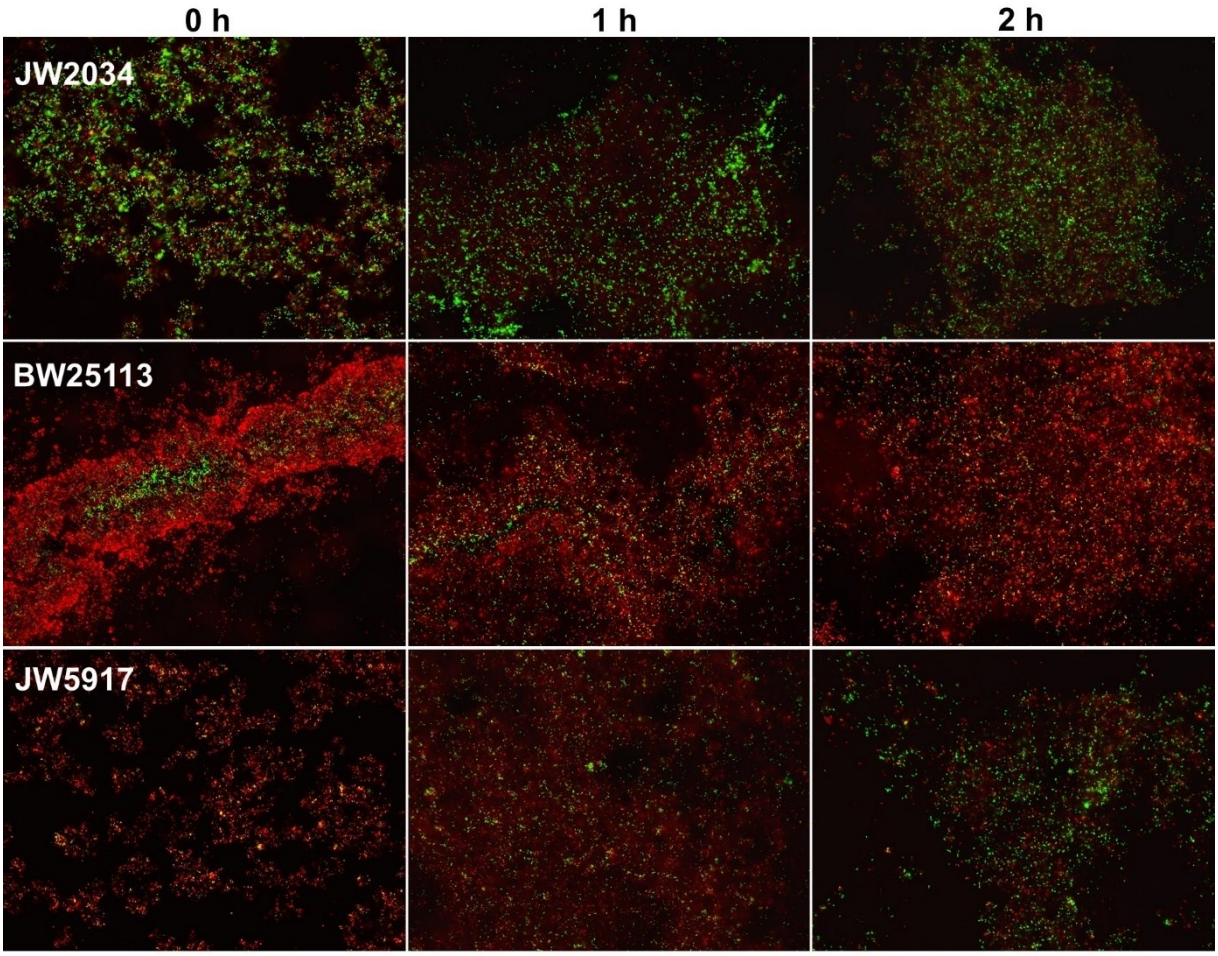

Figure S9. Fluorescent images of *E. coli* cells after 30 min of nZVI inactivation and subsequent incubation in LB medium for different duration to repair the damaged cell membrane.

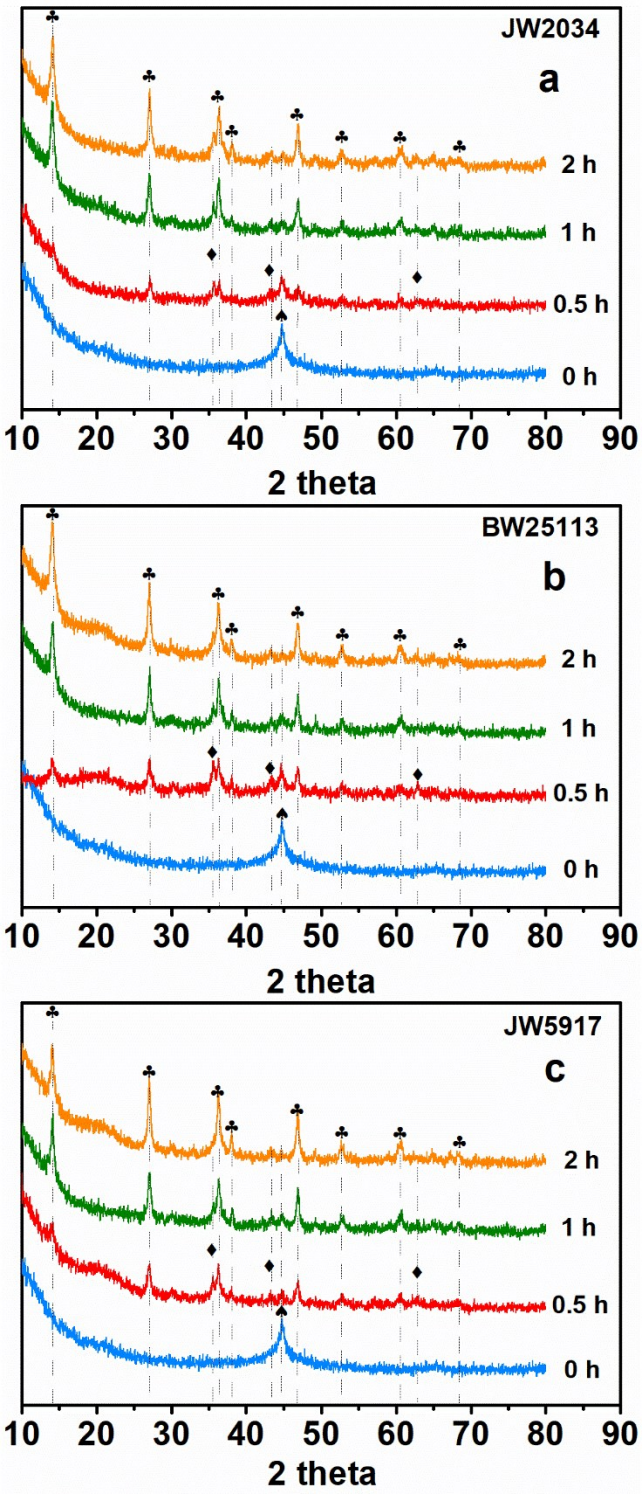

Figure S10. XRD patterns of nZVI samples collected from nZVI-*E. coli* systems after different durations. (a) JW2034, (b) BW25113, (c) JW5917. The spade (♠) indicates the diffraction peak of Fe^0 (JCPDS: 87-722), diamonds (♦) represented the peaks of magnetite (Fe_3O_4, JCPDS: 89-4319) and clubs (♣) stand for the peaks of lepidocrocite (γ-FeO(OH), JCPDS: 08-0098). nZVI dose is 500 mg/L.

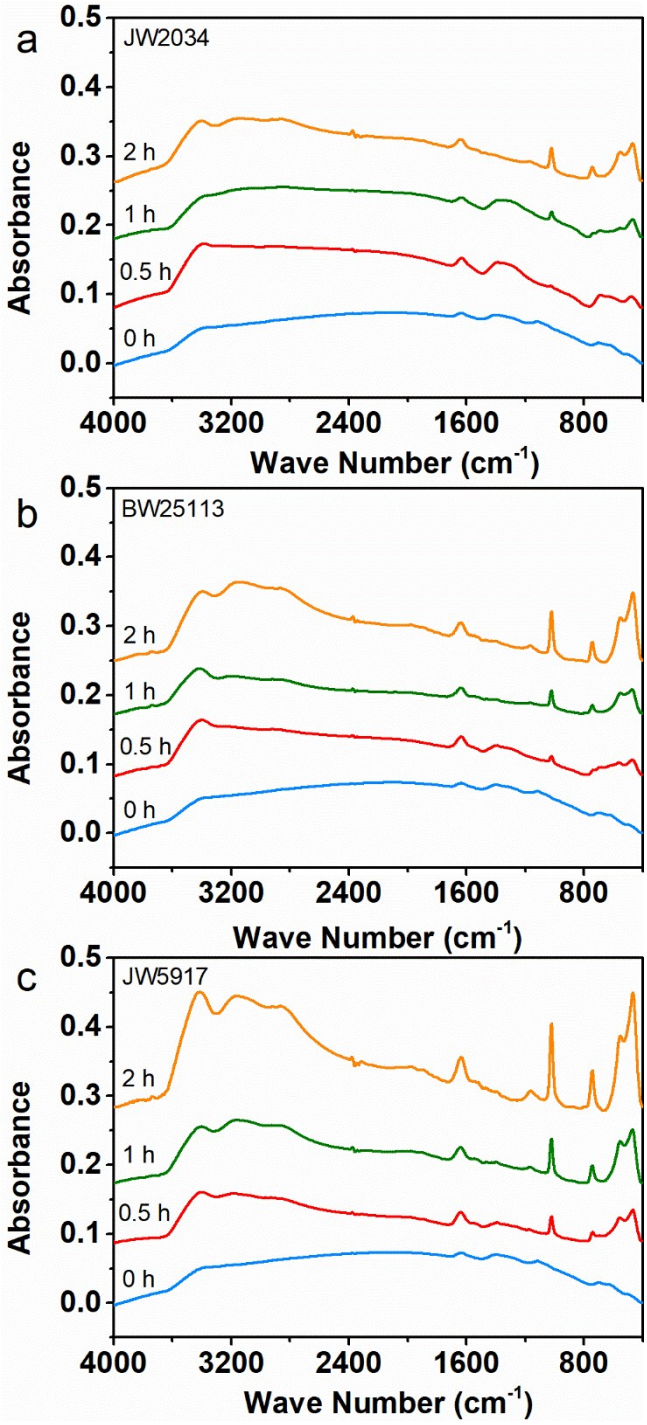

Figure S11. FT-IR spectra of the nZVI samples collected after different time of contact with *E. coli* (a) JW2034, (b) BW25113 and (c) JW5917. nZVI dose is 500 mg/L.

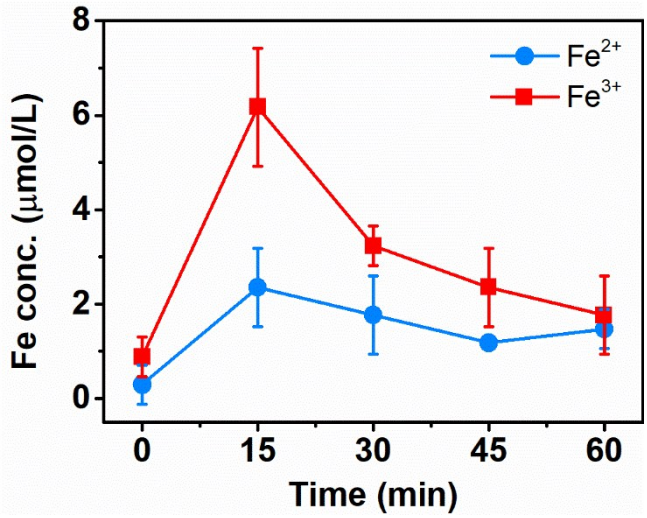

Figure S12. Concentrations of Fe^{2+} and Fe^{3+} released by the dissolution of nZVI.

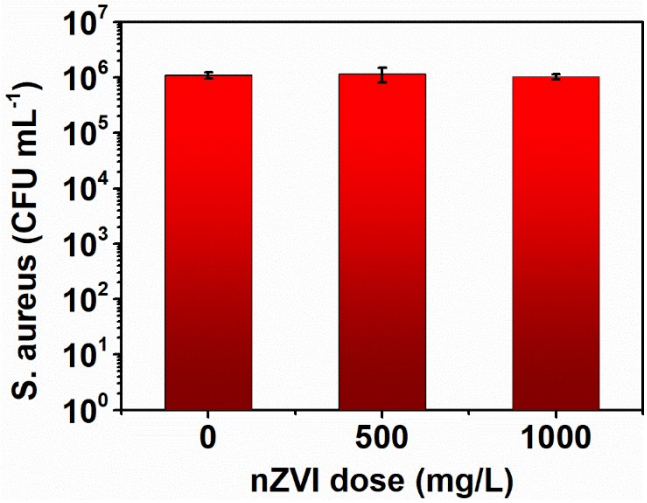

Figure S13. Concentrations of *S. aureus* after 1 h of aerobic nZVI inactivation at different doses. Initial concentration of *S. aureus* suspension used was approximate 10^6 CFU mL^{-1}.

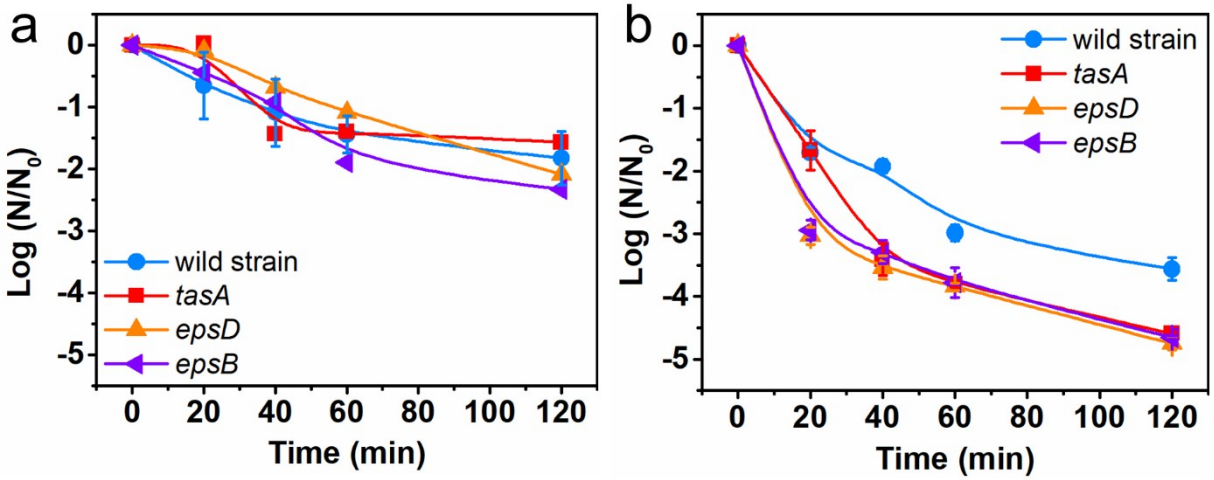

Figure S14. Aerobic inactivation of *Bacillus subtilis* (a) in the absence of nZVI and (b) in the presence of 500 mg/L nZVI. The initial concentrations of *Bacillus subtilis* were approximate 10^7 CFU mL^{-1}.

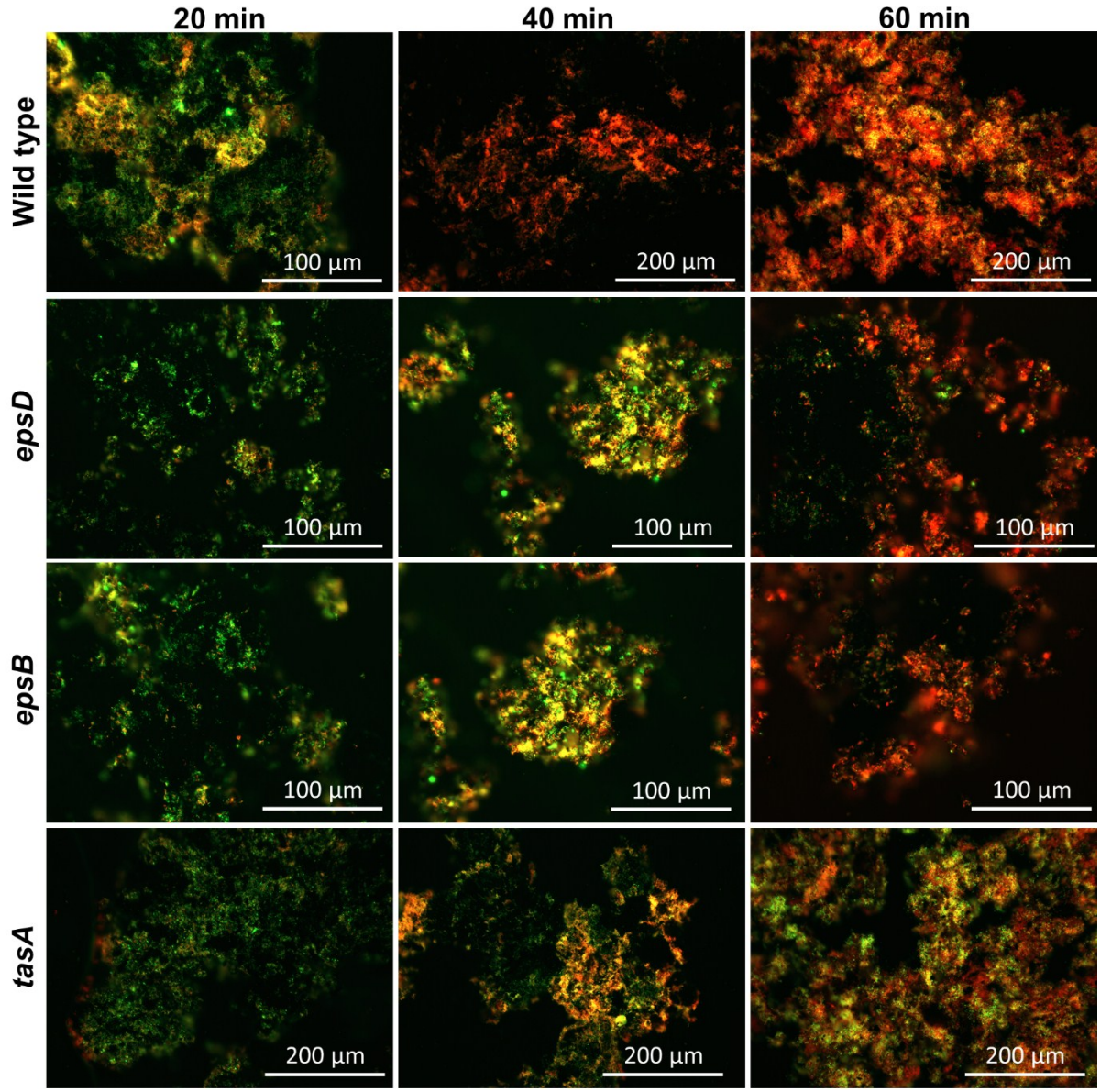

Figure S15. Fluorescent images of *Bacillus subtilis* wild type strain and mutant strains taken at different inactivation duration with 500 mg/L nZVI.

Table S1. Bacillus subtilis strains used in this study

CCTCC No.[a]	NBRP No.[b]	Disrupted Gene	Gene products or function
1542C0001AB130001	MGNA-A001	Wild strain	
1542C0001AB130044	MGNA-A044	*tasA*	major component of biofilm matrix, forms amyloid fibers
1542C0001AB130070	MGNA-A070	*epsD*	extracellular polysaccharide synthesis
1542C0001AB130072	MGNA-A072	*epsB*	extracellular polysaccharide synthesis, protein tyrosine kinase

[a] CCTCC: China Center for Type Culture Collection

[b] NBRP: National BioResource Project, Japan

Table S2. Ratios of *E. coli* cells with different membrane integrity, after different nZVI treatment duration, determined by using LIVE/DEAD™ BacLight™ Bacterial Viability Kit staining and flow cytometry.

E. coli	Time (min)	Intact	Permeable	Partially permeable
BW25113	15	32.6 ± 4.4%	19.9 ± 3.4%	47.5 ± 1.0%
	30	35.3 ± 2.3%	25.3 ± 2.0%	39.3 ± 0.3%
	45	28.1 ± 9.1%	25.2 ± 3.1%	46.7 ± 6.1%
	60	25.7 ± 2.2%	31.5 ± 6.0%	42.9 ± 3.8%
JW2034	15	45.3 ± 0.1%	13.8 ± 1.0%	40.9 ± 1.1%
	30	40.3 ± 1.8%	23.4 ± 0.5%	36.3 ± 1.3%
	45	24.3 ± 0.7%	37.3 ± 1.7%	38.4 ± 2.4%
	60	26.0 ± 3.9%	42.1 ± 3.9%	31.9%
JW5917	15	17.5 ± 1.7%	36.0 ± 3.2%	46.5 ± 4.9%
	30	22.3 ± 3.6%	35.1 ± 1.5%	42.6 ± 2.1%
	45	16.5 ± 2.6%	44.3 ± 4.8%	39.3 ± 2.2%
	60	14.9 ± 4.2%	49.1 ± 7.1%	35.9 ± 2.8%